

Reaction of $(\text{Me}_3\text{SiNSN})_2\text{S}$ with palladium complexes; crystal structures of $[\text{PPh}_4]_2[\text{Pd}_2\text{Br}_4(\text{S}_3\text{N}_2)]$ and $[\text{PPh}_4][\text{PdBr}_2(\text{S}_2\text{N}_3)]$

Paul F Kelly,* Alexandra M. Z. Slawin and Antonio Soriano-Rama

Department of Chemistry, Loughborough University of Technology, Loughborough LE11 3TU, UK

Reaction of $\text{Me}_3\text{SiNSNSNSNSiMe}_3$ with $[\text{PPh}_4]_2[\text{Pd}_2\text{Cl}_6]$ resulted in a mixture of $[\text{PPh}_4][\text{PdCl}_2(\text{S}_2\text{N}_3)]$ and $[\text{PPh}_4]_2[\text{Pd}_2\text{Cl}_4(\text{S}_3\text{N}_2)]$; in addition to the analogous bromo species, reaction with $[\text{PPh}_4]_2[\text{Pd}_2\text{Br}_6]$ also generated $[\text{PPh}_4]_2[\text{Pd}_2\text{Br}_6(\text{S}_2\text{N}_2)]$. The crystal structure of $[\text{PPh}_4][\text{PdBr}_2(\text{S}_2\text{N}_3)]$, only the second full characterization of a complex of $[\text{S}_2\text{N}_3]^-$, confirmed the presence of two distinct S–N bond lengths (1.49 and 1.6 Å), while the ^{15}N NMR spectrum of partially ^{15}N -labelled $[\text{PPh}_4][\text{PdCl}_2(\text{S}_2\text{N}_3)]$ confirms the absence of protonation on the S–N ligand. Potential mechanisms for these reactions are discussed.

The continued interest in the co-ordination chemistry of sulfur–nitrogen ligands is testimony to the ability of the resulting complexes to exhibit a range of bonding modes and structural properties.¹ A good example of such a ligand type is the bidentate S_2N_3 unit. This exists, formally as $[\text{S}_2\text{N}_3]^{3-}$, in complexes of the early transition metals, and as $[\text{S}_2\text{N}_3]^-$ in a recently reported palladium complex, $[\text{PPh}_4][\text{PdCl}_2(\text{S}_2\text{N}_3)]$.² The latter is formed, in low yield, by reaction of S_5N_6 with $[\text{PPh}_4]_2[\text{Pd}_2\text{Cl}_6]$. The use of S_5N_6 has a serious drawback as this sulfur nitride is, if anything, even more explosive than species such as S_4N_4 (which itself requires careful handling) and is, unlike the latter, extremely air-sensitive. Indeed, this combination of undesirable properties is the most likely reason why the aforementioned reaction marks the first (and thus far only) synthetic use of S_5N_6 .

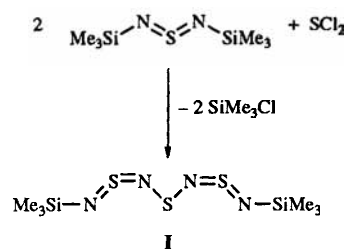
By far the most commonly used starting material for the preparation of metal sulfur–nitrogen complexes is S_4N_4 , which reacts with a wide range of transition-metal species; other compounds such as $(\text{NSCl})_3$ have also found use. Here we report on reactions of the sulfur–nitrogen chain species $\text{Me}_3\text{SiNSNSNSNSiMe}_3$ **I** (Scheme 1), a compound which has been known for some time³ but which has received little attention with respect to its reactivity towards transition-metal complexes. Reactions with $[\text{PPh}_4]_2[\text{Pd}_2\text{X}_6]$ ($\text{X} = \text{Cl}$ or Br) proceed in subtly different ways, depending upon the halogen present, and lead to a number of species including complexes of $[\text{S}_2\text{N}_3]^-$. This preparation of the latter has the advantage of circumventing the pernicious properties of S_5N_6 , as the starting material is now neither explosive nor air-sensitive.

Experimental

Unless stated otherwise all reactions were performed under an inert atmosphere (N_2) using standard Schlenk techniques. Solvents were dried and distilled before use: toluene from Na, Et_2O from sodium–benzophenone and CH_2Cl_2 from calcium hydride. Infrared spectra were recorded as KBr discs using a PE 2000 FT IR spectrometer, ^1H and ^{31}P NMR spectra on a JEOL FX90Q machine operating at 89.55 and 36.21 MHz respectively and ^{15}N spectra on a JEOL JNM EX270 spectrometer at 27.38 MHz. Microanalysis was performed by the LUT chemistry departmental service. The compound $\text{Me}_3\text{SiNSNSiMe}_3$ was made by the literature route.⁴

$(\text{Me}_3\text{SiNSN})_2\text{S}$ **I**

A solution of freshly distilled SCl_2 (2.35 g, 23.03 mmol) in CH_2Cl_2 (5 cm^3) was added dropwise to a stirred solution of



Scheme 1

$\text{Me}_3\text{SiNSNSiMe}_3$ (9.59 g, 46.12 mmol) in CH_2Cl_2 (20 cm^3) with the reaction flask immersed in a solid CO_2 –acetone bath (-78°C). Once the addition was complete the deep blue suspension was stirred for 60 min and the flask then allowed to warm to room temperature. The resulting mixture was filtered through Celite and the red solution concentrated *in vacuo*. The red oil was dissolved in hexane and filtered through Celite, in air, to remove any traces of S_4N_4 . The red filtrate was concentrated and then the oil exposed to air on a watch-glass overnight to give large orange needles of compound **I** (yield 2.36 g, 34.4%). Infrared, ^1H NMR and mass spectral data were in accord with the literature values.³

$[\text{PPh}_4]_2[\text{Pd}_2\text{Cl}_6]$ **1a**

A mixture of PdCl_2 (0.81 g, 4.6 mmol) and NaCl (0.53 g, 9.1 mmol) in distilled water (100 cm^3) was stirred at 70°C for 90 min. The resulting dark solution was treated with $[\text{PPh}_4]\text{Cl}$ (1.71 g, 4.6 mmol) dissolved in water (50 cm^3), giving a brown precipitate which was collected and recrystallized from CH_2Cl_2 –toluene (yield 1.85 g, 73%).

$[\text{PPh}_4]_2[\text{Pd}_2\text{Br}_6]$ **1b**

A mixture of PdCl_2 (0.31 g, 1.8 mmol) and KBr (0.84 g, 7.1 mmol) was stirred in distilled/degassed water (100 cm^3) at 60°C for 90 min. The resulting wine-coloured solution was treated with $[\text{PPh}_4]\text{Br}$ (0.74 g, 1.8 mmol) dissolved in water (50 cm^3) to give a brown precipitate which was collected, in air, and then recrystallized from CH_2Cl_2 –toluene (yield 1.02 g, 79%).

Reaction of compound **I** with $[\text{PPh}_4]_2[\text{Pd}_2\text{Cl}_6]$

A solution of $[\text{PPh}_4]_2[\text{Pd}_2\text{Cl}_6]$ (110 mg, 0.1 mmol) in CH_2Cl_2 (150 cm^3) was treated with solid compound **I** (59 mg, 0.2 mmol), giving a brown solution which was stirred for 90 min. The volume of the solution was reduced to a few cm^3 *in vacuo* and

layered with Et₂O. Slow diffusion for 48 h resulted in the growth of black material, as both well formed plates and a mass of microcrystals, together with a very small crop of orange needles. These were separated from each other manually. Infrared spectroscopy showed the black plates and microcrystals to be [PPh₄][PdCl₂(S₂N₃)] **2a**, yield 45 mg (36% based on palladium) (Found: C, 45.4; H, 3.1; N, 6.2. Calc for C₂₄H₂₀Cl₂N₃PPdS₂: C, 46.3; H, 3.2; N, 6.7%) and the orange crystals to be [PPh₄]₂[Pd₂Cl₄(S₃N₂)] **3a**.

Reaction of compound I with [PPh₄]₂[Pd₂Br₆]

A solution of [PPh₄]₂[Pd₂Br₆] (150 mg, 0.1 mmol) in CH₂Cl₂ (150 cm³) was treated with solid compound I (65 mg, 0.2 mmol), giving a dark red solution which was stirred for 90 min. The solution was reduced to a few cm³ *in vacuo* and layered with Et₂O. Slow diffusion for 48 h resulted in the growth of three types of crystals: black three-dimensional prisms, brown plates and orange flakes. These were separated from each other manually. Infrared spectroscopy (Table 1) showed the orange and brown crystals to be [PPh₄]₂[Pd₂Br₆(S₃N₂)] **3b** (yield *ca.* 5 mg) and [PPh₄]₂[Pd₂Br₆(S₂N₂)] **4** (yield 20 mg, 13% based on palladium) respectively. X-Ray crystallography revealed the black crystals to be [PPh₄][PdBr₂(S₂N₃)] **2b**, yield 60 mg (38% based on palladium) (Found: C, 40.2; H, 2.7; N, 5.3. Calc for C₂₄H₂₀Br₂N₃PPdS₂: C, 40.5; H, 2.8; N, 5.9%).

Partially ¹⁵N-labelled complex 2a

Reaction of 66% ¹⁵N-labelled S₅N₆ (67 mg, 0.27 mmol), itself prepared by the reaction of S₄¹⁵N₄Cl₂ with Me₃SiNSNSiMe₃,⁵ with [PPh₄]₂[Pd₂Cl₆] (147 mg, 0.13 mmol) in CH₂Cl₂ (30 cm³), followed by stirring overnight, resulted in a red solution. This was reduced in volume to a few cm³, slow diffusion of diethyl ether resulted in a mixture of crystals from which the very dark samples of complex **2a** were separated and their ¹⁵N NMR spectrum recorded.

Reaction of compound I with [Pt(PPh₃)₃]

A solution of compound I (30 mg, 0.1 mmol) in toluene (10 cm³) was added to a solution of [Pt(PPh₃)₃] (100 mg, 0.1 mmol) in the same solvent (50 cm³) to give a green solution, which turned pale brown within 10 min. After stirring for 1 h the solvent was removed *in vacuo* to yield a brown solid. Addition of CH₂Cl₂ to the solid resulted in a suspension of a red solid in a yellow solution, which was filtered. Infrared spectroscopy showed the red solid to be [Pt(S₂N₂)(PPh₃)₂]₂⁶ (yield 8 mg, 14%). The volume of the yellow filtrate was reduced to 5 cm³ *in vacuo* and a yellow solid precipitated by addition of hexane, leaving only PPh₃ (as shown by ³¹P NMR spectroscopy) in solution. Infrared and ³¹P NMR measurements revealed the yellow solid to be [Pt(S₂N₂)(PPh₃)₂]₂⁷ yield 48 mg (58%) [³¹P: δ_A 11.5, ¹J(¹⁹⁵Pt-³¹P_A) 2995; δ_X 24.1, ¹J(¹⁹⁵Pt-³¹P_X) 2825 Hz]. Essentially the same products were formed when the reaction was performed at a 2:1 I:Pt ratio.

Reaction of complex 2b with dppe

A mixture of complex **2b** (20 mg, 0.03 mmol) and dppe (Ph₂PCH₂CH₂PPh₂) (11 mg, 0.03 mmol) was dissolved in dry CDCl₃ (4 cm³) giving a pale orange solution. The ³¹P NMR spectrum of this solution showed, in addition to [PPh₄]⁺ cation, the presence of [Pd(dppe)Br₂] (δ 64.4) and [Pd-(S₂N₂)(dppe)] [δ_A 55.1, δ_X 48.5; ²J(³¹P-³¹P) 26 Hz].

X-Ray crystallography

Crystal data for complex 2b. C₂₄H₂₀Br₂N₃PPdS₂, *M* = 711.74, monoclinic, space group *P*2₁/*n*, *a* = 13.294(2), *b* =

14.138(2), *c* = 13.927(2) Å, β = 99.51(1)°, *U* = 2581.4(6) Å³, *Z* = 4, *D*_c = 1.83 g cm⁻³, dark needle of dimensions 0.08 × 0.1 × 0.3 mm, μ(Cu-Kα) = 116.6 cm⁻¹, λ = 1.541 78 Å, *F*(000) = 1392.

All measurements were made on a Rigaku AFC7S diffractometer with graphite-monochromated Cu-Kα radiation using the ω-2θ scan technique to a maximum 2θ value of 110°. Of 3405 measured reflections 3235 were unique [*I* > 3σ(*I*)]. Data were corrected for Lorentz and polarization effects and an empirical absorption correction was applied resulting in transmission factors ranging from 0.65 to 0.99.

Crystal data for complex 3b. C₄₈H₄₀Br₄N₂P₂Pd₂S₃·C₂, *M* = 1359.42, monoclinic, space group *P*2₁/*n*, *a* = 10.445(4), *b* = 12.966(4), *c* = 41.403(4) Å, β = 93.96(2)°, *U* = 5593(2) Å³, *Z* = 4, *D*_c = 1.61 g cm⁻³, orange needle of dimensions 0.09 × 0.11 × 0.23 mm, μ(Cu-Kα) = 103.74 cm⁻¹, λ = 1.541 78 Å, *F*(000) = 2656.

All measurements were made as for complex **2b**. Of 6534 measured reflections 6108 were unique [*I* > 3σ(*I*)]. Data were corrected as for **2b**; transmission factor range 0.62–1.00.

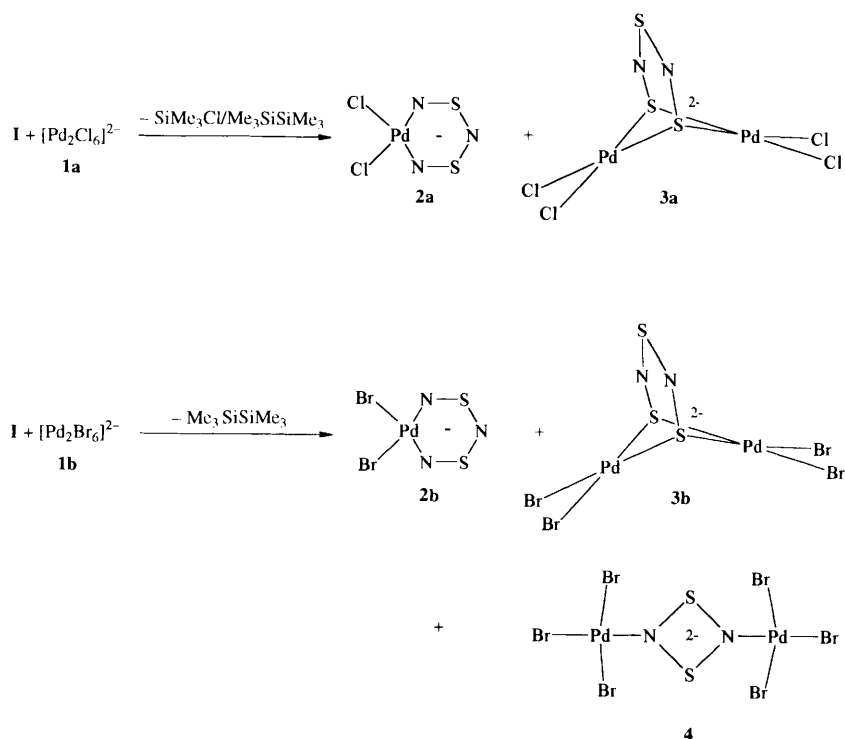
Structure analysis and refinement. The structures were solved by heavy-atom Patterson methods and expanded using Fourier techniques. The phenyl rings in both structures were refined as rigid bodies with overall *B* factors; all other non-hydrogen atoms were refined anisotropically. In complex **3b** four unidentified solvent sites were located from a Δ*F* map. These were refined isotropically as half weight carbons, but could not be resolved into meaningful fragments. This, along with poor crystal quality, is reflected in the high *R* factor. Hydrogen-atom coordinates were refined but their isotropic *B* values were held fixed. Refinement was by full-matrix least squares to *R* = 0.060 (**2b**) and 0.086 (**3b**) [*R* = Σ(|*F*_o| - |*F*_c|)/Σ|*F*_o|], *R*' = 0.051 and 0.101 respectively {*R*' = [Σw(|*F*_o| - |*F*_c|)²/Σ(w*F*_o)²]^{1/2} with *w* = 1/σ²(*F*)}. The maximum and minimum residual electron densities in the final Δ*F* map were 1.09 and -0.99 (**2b**) and 1.11 and -1.91 e Å⁻³ (**3b**), while the maximum shifts/error in the final refinement cycle were 0.04 and 0.71 for **2b** and **3b** respectively. All calculations were performed using the TEXSAN crystallographic software package.⁸

Complete atomic coordinates, thermal parameters and bond lengths and angles have been deposited at the Cambridge Crystallographic Data Centre. See Instructions for Authors, *J. Chem. Soc., Dalton Trans.*, 1996, Issue 1.

Results and Discussion

It has been known for some time that Me₃SiNSNSiMe₃ reacts with 0.5 equivalents of SCl₂ to give the long-chain analogue Me₃SiNSNSNSiMe₃ *via* loss of 2 equivalents of SiMe₃Cl (Scheme 1).³ The reaction is not particularly efficient (our typical yield is *ca.* 34%), due to the production of large amounts of (SN)_x as by-product. It can, however, be performed on a reasonably large scale, allowing the isolation (see Experimental section) of multigram quantities of **I** as well formed dark-orange needles.

We have previously demonstrated the usefulness of the halide-bridged palladium(II) dimers [Pd₂Cl₆]²⁻ **1a** and [Pd₂Br₆]²⁻ **1b** in the preparation of sulfur-nitrogen complexes;⁹ we have now found they readily react with compound **I** to give a variety of species. Thus addition of solid **I** to a solution of **1a** in CH₂Cl₂ results in a dark coloured mixture; if, after a few hours stirring, diethyl ether is layered on this solution, slow diffusion over the next 1–2 d yields dark crystals. Microanalysis and IR spectroscopy (Table 1) reveal this product to be [PPh₄][PdCl₂(S₂N₃)] **2a** (Scheme 2). In addition a very small yield of orange crystals is also obtained; these are formed in somewhat larger yield if either (a) the above



Scheme 2 Products of the reaction of compound **I** with complexes **1a** and **1b**

crude product mixture (including material which did not form well defined crystals) is recrystallized or (b) the initial reaction mixture is left to stir for a few days before crystallization. Infrared spectroscopy reveals this compound to be $[\text{PPh}_4]_2\text{-}[\text{Pd}_2\text{Cl}_4(\text{S}_2\text{N}_2)]$ **3a**. As Scheme 2 also shows, if the reaction is performed in CD_2Cl_2 then *in situ* ^1H NMR spectroscopy reveals the presence of SiMe_3Cl and $\text{Me}_3\text{SiSiMe}_3$ in the reaction mixture.

In the case of the reaction of S_2N_4 with the palladium dimers, changing from the chloro species to the bromo does not appear to make any significant difference to the progress of the reaction. This is not the case with reactions of compound **I**, however. Here we find that reaction of **I** and **1b**, as above, followed by diffusion of ether, leads to a high yield of a mixture of $[\text{PPh}_4][\text{PdBr}_2(\text{S}_2\text{N}_3)]$ **2b** and the S_2N_2 adduct $[\text{PPh}_4]_2\text{-}[\text{Pd}_2\text{Br}_6(\text{S}_2\text{N}_2)]$ **4** (Scheme 2). Again, if the mixture is left longer before crystallization then significant amounts of $[\text{PPh}_4]_2\text{-}[\text{Pd}_2\text{Br}_4(\text{S}_3\text{N}_2)]$ **3b** form. Another contrast to the chloro reaction comes with the ultimate fate of the trimethylsilyl groups; in this case only $\text{Me}_3\text{SiSiMe}_3$ is formed (*i.e.* no SiMe_3Br) (Scheme 2).

As preparative routes to the $[\text{S}_2\text{N}_3]^-$ complexes the above reactions have a number of distinct advantages over the only previously reported route. The primary advantage comes in the form of the S–N starting material which in this case is neither particularly air-sensitive nor explosive (in stark contrast to S_5N_6 which is made difficult to handle on both these fronts). In addition, the yields are higher (*ca.* 40% based on Pd) and significantly more reproducible.

As for the mechanisms of the reactions, any explanation of how the reactions of complexes **1a** and **1b** proceed must account for the different products shown in Scheme 2. Monitoring the reactions to try to determine these mechanisms is hindered by the lack of NMR-active nuclei in the ultimate products; specifically it is difficult to envisage a realistic preparative route to ^{15}N -labelled **I**, and hence we cannot use ^{15}N NMR spectroscopy to probe intermediates (as was the case in the reactions of S_4N_4 ,⁹ which is amenable to nitrogen-15 enrichment, with **I**). We can, of course, monitor the progress of the degradation of **I** by ^1H NMR spectroscopy; Fig. 1 contrasts

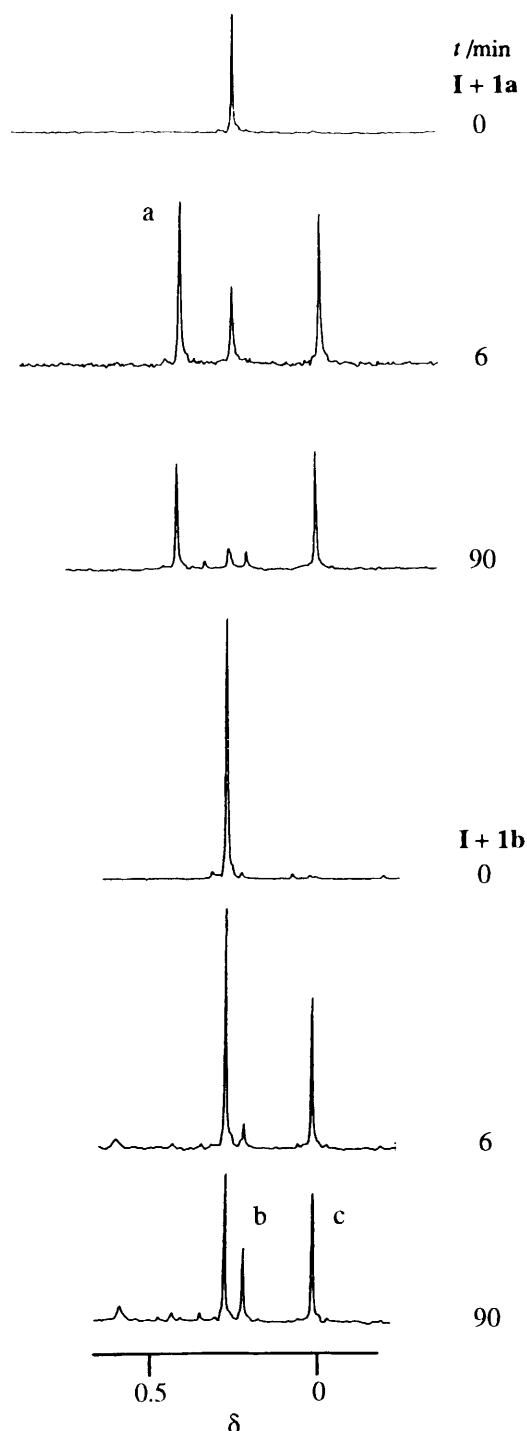
the two reactions. In the case of **1a** it can be seen that 6 min after mixing some 80% or so of **I** (δ 0.29) has reacted; by 90 min only a trace remains, together with a trace of $\text{Me}_3\text{SiNSNSiMe}_3$ (δ 0.24). By this stage there has effectively been complete conversion of the Me_3Si groups in **I** into SiMe_3Cl (δ 0.42) and $\text{Me}_3\text{SiSiMe}_3$ (δ 0.06) (molar ratio 2:1). The degradation of **I** in the reaction with **1b** is clearly slower. After 6 min just over half of the compound is still intact; appreciable amounts of $\text{Me}_3\text{SiSiMe}_3$ are present together with a small amount of $\text{Me}_3\text{SiNSNSiMe}_3$. After 90 min **I** is still the predominant species, with $\text{Me}_3\text{SiNSNSiMe}_3$ present in significant amounts. Overnight reaction sees only $\text{Me}_3\text{SiSiMe}_3$ remain. So whereas dimer **1a** reacts with both equivalents of **I** in a matter of minutes, **1b** appears to use up only 1 equivalent on that time-scale, with the final equivalent taking many hours to react.

In the case of complex **1a** the above observations suggest that 2 equivalents of **I** react with a dimer to generate 2 mol of an adduct of the type $[\text{PdX}_3\text{-I}]^-$. Clearly, this adduct is short lived (as no Me_3Si peaks associated with it are seen) and, given the preponderance of nitrogen-bound products eventually formed in these reactions, could well involve co-ordination *via* nitrogen (Scheme 3). Reaction of one of the Me_3Si groups with a metal-halide bond would release the observed SiMe_3Cl ; subsequent degradation of the resulting species to **2a** could then be achieved by loss of a Me_3Si unit (as half a mole of $\text{Me}_3\text{SiSiMe}_3$) and the residual S–N fragment (presumably, ultimately, as S_4N_4 ; the latter is indeed observed in the crude reaction mixture by IR spectroscopy).

In contrast, reaction of compound **I** with **1b** gives a subtly different break-up of the original dimer; in this case we believe the initial products are a bidentate adduct of the type $[\text{PdX}_2\text{-I}]$, which could clearly act as a source of **2b**, and the tetrabromo dianion $[\text{PdBr}_4]^{2-}$ (Scheme 3). The latter can be readily detected in the reaction mixture. Comparison of the IR spectrum of the solid obtained by evaporation of the reaction mixture after 1 h with that of $[\text{PPh}_4]_2[\text{PdBr}_4]$ reveals a clear correlation of the Pd–Br stretch at 247 cm^{-1} , indicative of $[\text{PdBr}_4]^{2-}$ (the IR spectrum of **2b** shows two bands in this area, at 239 and 256 cm^{-1}). This explains why the ^1H NMR results are as seen; 1 equivalent of **I** will be used up very quickly by

Table 1 Infrared data (cm⁻¹) for complexes **2–4** (literature values in parentheses)

[PPh ₄][PdCl ₂ (S ₂ N ₃)] 2a	[PPh ₄][PdBr ₂ (S ₂ N ₃)] 2b	[PPh ₄] ₂ [Pd ₂ Cl ₄ (S ₃ N ₂)] 3a	[PPh ₄] ₂ [Pd ₂ Br ₄ (S ₃ N ₂)] 3b	[PPh ₄] ₂ [Pd ₂ Br ₆ (S ₂ N ₂)] 4
858vs (858) ²	857s	643m (643) ⁹	641m (642) ⁹	867m (868) ⁹
675 (sh)	671 (sh)	386w (387)	381m (383)	432m (434)
408m (409)	510 (sh)	309w (309)	251w (251)	257m (265)
307m (308)	401w	290w (291)		249m (251)
	317w			

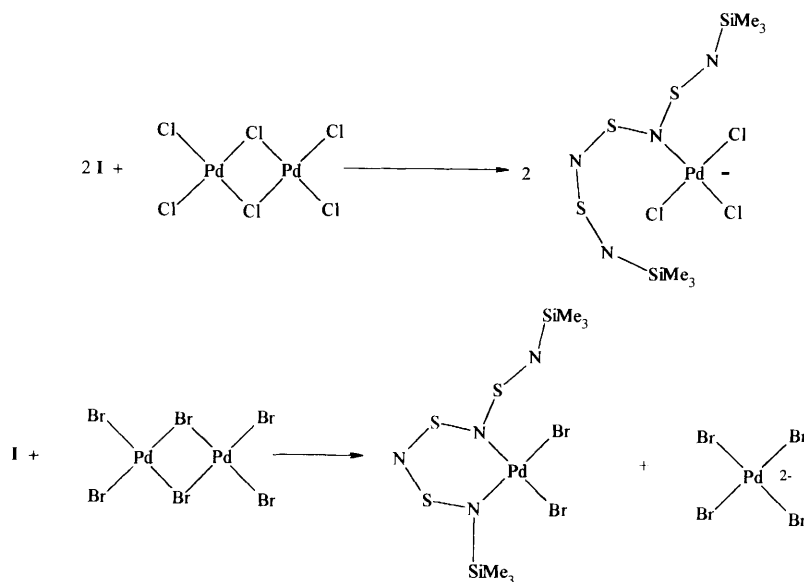
**Fig. 1** Comparison of the change with time of the ¹H NMR spectra of solutions of compound **I** with complexes **1a** and **1b** in CD₂Cl₂. Peaks: a, SiMe₃Cl; b, Me₃SiNSNSiMe₃; c, Me₃SiSiMe₃

reaction with the dimer, but the second will only be used up in the reaction with [PdBr₄]²⁻, which would be expected to be markedly slower. If a sample of pure [PPh₄]₂[PdBr₄] is treated

with **I** a mixture of **4** and some **2b** is obtained, indicating that the presence of [PdBr₄]²⁻ is indeed crucial to the formation of **4**. It is noteworthy that in the reaction of **I** with **1b**, where large amounts of the S₂N₂ adduct result. Me₃SiNSNSiMe₃ is also formed as the reaction proceeds. Given that removal of a neutral S₂N₂ unit from **I** would leave Me₃SiNSNSiMe₃, we can conclude that at some point an adducted molecule of **I** undergoes cleavage to these two products.

The presence of compounds **3** in the product mixtures clearly indicates that the above mechanistic arguments do not tell the whole story. In previous work we explained the appearance of the latter in the reactions of **I** with S₄N₄ by proposing a palladium(IV) intermediate containing the [S₄N₄]²⁻ ligand.⁹ It may be that adducts initially formed as in Scheme 3 can undergo redox reactions to give unstable palladium(IV) species which then decompose back to Pd^{II} with disruption of the ligand. It is also possible that some amounts of sulfur-bound adducts form in the initial reaction and then react further to give **3**; or that the sulfur–nitrogen fragments lost as S₄N₄ in the final degradation of the species in Scheme 3 react to give **3** (although this is less likely, as one would expect to see the chloro equivalent of **4** forming from **1a**). The fact that more **3** appears to form with time suggests that it results from the degradation of an as yet unidentified intermediate. The latter must not contain Me₃Si groups (as these would be seen by NMR spectroscopy) and does not readily crystallize; this observation might suggest that it is neutral *i.e.* does not have the [PPh₄]⁺ cation, which tends to impart a greater ease of crystallization, present. One result of this mode of formation of **3b** is that crystalline samples are formed as needles rather than the thin plates observed previously (or obtained upon recrystallization of these samples). Clearly, the decomposition of the intermediate plays an important role during crystallization and imparts this different crystal form; the crystals formed in this way are amenable to X-ray crystallography (unlike the plate type), and this technique confirms the binuclear structure of the anion (Fig. 2). Comparing this structure to that of **3a** reveals little difference in the important S–N bond lengths and angles (Tables 2 and 3).

The crystal structure of complex **2b** (Fig. 3, Tables 4 and 5) reveals bond distances and angles similar to those reported for **2a**, with the anion essentially planar [maximum deviation from the mean plane at S(1), –0.13 Å]. Comparison of these two sets of values with those for early transition-metal complexes of the [S₂N₃]³⁻ ligand reveals an interesting contrast. In the latter the average S–N (metal-bound) and S–N (bridgehead) lengths are fairly similar. Thus for the complexes [MoCl₄(S₂N₃)]⁻, [WCl₄(S₂N₃)]⁻ and [WCl₃(S₂N₃)(MeCN)] these average out as 1.57 and 1.59 Å respectively.¹ In complexes **2a** and **2b** however, these values average out as 1.49 and 1.60 Å, indicating a significant difference in the bonding arrangement. When we first reported the preparation of **2a** we noted that the apparent absence of N–H stretches in the IR spectrum ruled out the possibility that the ligand was actually a protonated version of [S₂N₃]³⁻ (a possibility not unambiguously dealt with by X-ray crystallography). We now have absolute proof that the ligand is not protonated, by virtue of the ¹⁵N NMR spectrum of partially labelled **2a**. The latter may be prepared by the reaction of 66% labelled S₅N₆ (prepared by the reaction of S₄¹⁵N₄Cl₂



Scheme 3 Comparison of proposed intermediates in the reaction of compound **I** with complexes **1a** and **1b**

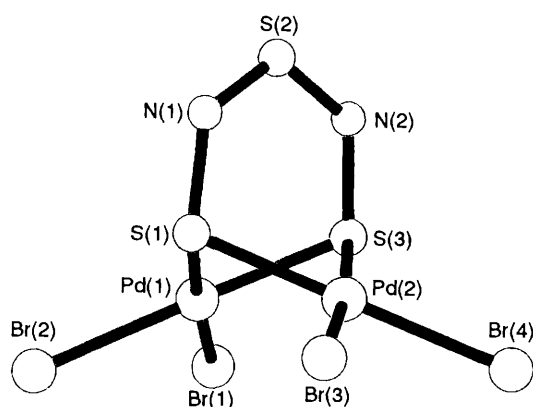


Fig. 2 Crystal structure of the anion in complex **3b**

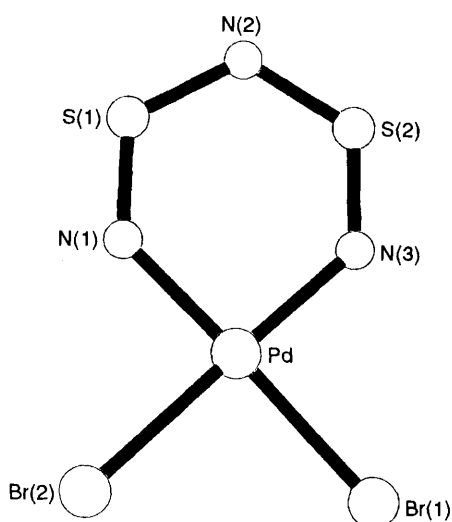


Fig. 3 Crystal structure of the anion in complex **2b**

with $\text{Me}_3\text{SiNSNSiMe}_3$) with **1a** (note that there is no obvious way to make labelled **I** in reasonable yield, thus making the use of S_5N_6 a necessity). As Fig. 4 shows, this spectrum consists of the expected two singlets, present in the ratio 2:1, at δ 460 (metal-bound) and 355 (bridgehead nitrogen). The key feature is that the spectrum is unchanged when run with or without proton decoupling. The presence of any protons on the nitrogens would invariably result in a substantial $^1J(\text{H}-^{15}\text{N})$ coupling in the latter case. It is also noteworthy that, in contrast

Table 2 Selected bond lengths (Å) and angles (°) in complex **3b**

Pd(1)–Br(1)	2.473(5)	Pd(1)–Br(2)	2.457(5)
Pd(1)–S(1)	2.279(12)	Pd(1)–S(3)	2.279(11)
S(1)–N(1)	1.652(34)	N(1)–S(2)	1.563(37)
S(2)–N(2)	1.605(51)	N(2)–S(3)	1.638(48)
Pd(2)–S(1)	2.280(12)	Pd(2)–S(3)	2.270(12)
Pd(2)–Br(3)	2.473(6)	Pd(2)–Br(4)	2.475(6)
Br(1)–Pd(1)–Br(2)	94.88(17)	Br(1)–Pd(1)–S(3)	91.27(32)
S(3)–Pd(1)–S(1)	85.37(41)	S(1)–Pd(1)–Br(2)	88.42(30)
Pd(1)–S(3)–Pd(2)	77.83(36)	Pd(1)–S(1)–Pd(2)	77.62(39)
Pd(1)–S(3)–N(2)	111.3(16)	Pd(1)–S(1)–N(1)	107.4(13)
S(3)–N(2)–S(2)	123.6(24)	N(2)–S(2)–N(1)	120.8(21)
S(2)–N(1)–S(1)	127.2(23)	Br(4)–Pd(2)–S(3)	89.04(35)
Br(4)–Pd(2)–Br(3)	96.56(21)	S(1)–Pd(2)–Br(3)	88.90(34)
S(3)–Pd(2)–S(1)	85.55(44)	Pd(2)–S(1)–N(1)	106.5(13)
Pd(2)–S(3)–N(2)	107.1(14)		

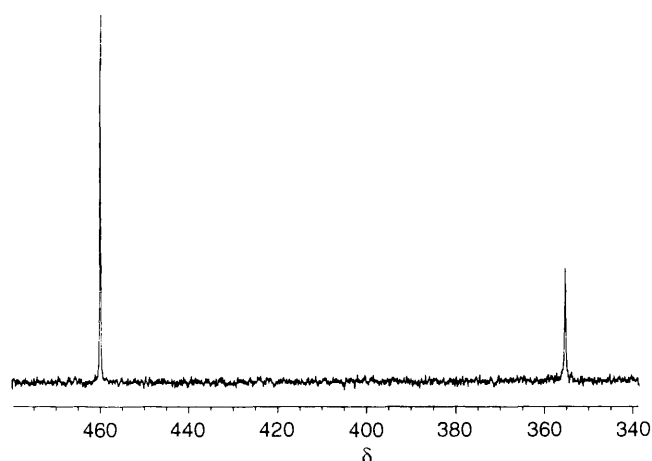


Fig. 4 The ^{15}N NMR spectrum of 66% ^{15}N -labelled complex **2a**

to some other metal sulfur–nitrogen complexes,¹⁰ there appear to be no resolvable $^2J(^{15}\text{N}-^{15}\text{N})$ interactions in this system.

The above reactions give us access to significant amounts of complexes of $[\text{S}_2\text{N}_3]^-$, giving the opportunity to study the chemistry of this ligand. Preliminary work in this area suggests that it is unstable with respect to a ring contraction to $[\text{S}_2\text{N}_2]^{2-}$. Thus reaction of complex **2b** with *dppe* results in a product mixture the ^{31}P NMR spectrum of which reveals, in addition to

Table 3 Atomic coordinates for complex **3b**

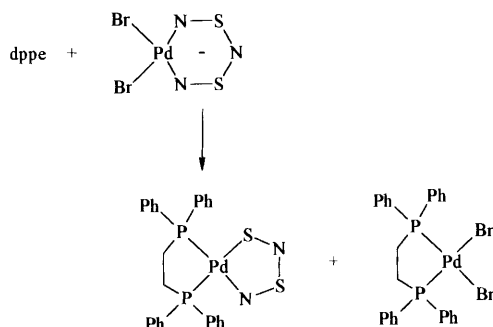
Atom	x	y	z	Atom	x	y	z
Pd(1)	0.001 6(3)	0.655 3(2)	0.582 04(7)	C(21)	0.062(3)	0.777(3)	0.728 3(9)
Pd(2)	-0.035 4(3)	0.776 9(2)	0.638 19(7)	C(22)	0.146(4)	0.855(3)	0.720 0(6)
Br(1)	-0.141 2(5)	0.515 6(4)	0.560 48(10)	C(23)	0.229(3)	0.900(2)	0.744(1)
Br(2)	0.026 2(5)	0.735 4(4)	0.529 05(10)	C(24)	0.228(3)	0.867(3)	0.775 9(8)
Br(3)	-0.030 0(5)	0.967 5(4)	0.640 5(1)	C(25)	0.609(3)	0.645(1)	0.471 4(6)
Br(4)	-0.219 0(5)	0.754 0(4)	0.672 2(1)	C(26)	0.737(2)	0.616(2)	0.476 3(5)
S(1)	0.130(1)	0.781 6(9)	0.604 9(3)	C(27)	0.775(2)	0.517(2)	0.467 8(5)
S(2)	0.250(1)	0.626(1)	0.646 4(4)	C(28)	0.684(3)	0.447(1)	0.454 4(5)
S(3)	-0.021(1)	0.602 8(9)	0.633 9(3)	C(29)	0.556(2)	0.476(2)	0.449 5(5)
P(1)	0.129(1)	0.765 4(9)	0.825 0(2)	C(30)	0.518(2)	0.575(2)	0.458 0(5)
P(2)	0.569(1)	0.774 1(8)	0.482 1(2)	C(31)	0.693(2)	0.858(2)	0.470 7(6)
N(1)	0.253(3)	0.724(3)	0.624 7(8)	C(32)	0.736(2)	0.846(2)	0.439 8(5)
N(2)	0.117(5)	0.569(3)	0.651 8(9)	C(33)	0.830(2)	0.912(2)	0.429 1(4)
C(1)	0.011(2)	0.847(2)	0.840 0(7)	C(34)	0.881(2)	0.990(2)	0.449 3(6)
C(2)	-0.012(3)	0.945(3)	0.826 8(5)	C(35)	0.838(2)	1.002(2)	0.480 2(5)
C(3)	-0.095(3)	1.013(2)	0.841 4(7)	C(36)	0.744(2)	0.937(2)	0.490 9(4)
C(4)	-0.154(2)	0.982(2)	0.869 0(7)	C(37)	0.554(2)	0.787(2)	0.524 1(4)
C(5)	-0.131(3)	0.885(3)	0.882 1(5)	C(38)	0.655(2)	0.749(2)	0.544 5(5)
C(6)	-0.048(3)	0.817(2)	0.867 6(7)	C(39)	0.652(2)	0.760(2)	0.578 0(5)
C(7)	0.280(2)	0.787(2)	0.847 4(6)	C(40)	0.548(2)	0.808(2)	0.591 0(4)
C(8)	0.284(2)	0.837(2)	0.877 4(6)	C(41)	0.447(2)	0.845(2)	0.570 6(6)
C(9)	0.401(3)	0.852(2)	0.895 1(4)	C(42)	0.450(2)	0.835(2)	0.537 1(5)
C(10)	0.514(2)	0.817(2)	0.883 0(6)	C(43)	0.419(2)	0.811(2)	0.461 2(5)
C(11)	0.510(2)	0.767(2)	0.853 0(6)	C(44)	0.417(2)	0.892(2)	0.438 8(6)
C(12)	0.393(3)	0.752(2)	0.835 3(4)	C(45)	0.301(2)	0.923(1)	0.423 2(5)
C(13)	0.076(4)	0.634(2)	0.829 3(7)	C(46)	0.187(2)	0.874(2)	0.429 9(5)
C(14)	0.163(2)	0.556(3)	0.838 4(6)	C(47)	0.189(2)	0.794(2)	0.452 3(5)
C(15)	0.122(3)	0.454(3)	0.839 2(6)	C(48)	0.305(3)	0.762(1)	0.467 9(5)
C(16)	-0.006(4)	0.430(2)	0.830 8(7)	C(49)	0.399(8)	0.334(7)	0.242(2)
C(17)	-0.093(2)	0.508(3)	0.821 7(6)	C(50)	0.401(7)	0.244(6)	0.232(2)
C(18)	-0.052(3)	0.610(2)	0.820 9(7)	C(51)	0.361(9)	0.172(8)	0.231(2)
C(19)	0.145(4)	0.789(3)	0.784 1(6)	C(52)	0.367(7)	0.071(6)	0.223(2)
C(20)	0.062(3)	0.744(2)	0.760(1)				

Table 4 Selected bond lengths (Å) and angles (°) in complex **2b**

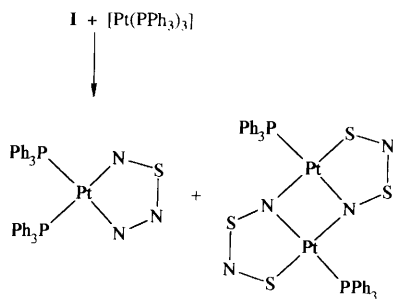
Pd–Br(1)	2.438(2)	Pd–Br(2)	2.461(2)
Pd–N(1)	1.921(12)	N(1)–S(1)	1.504(11)
S(1)–N(2)	1.607(13)	N(2)–S(2)	1.598(12)
S(2)–N(3)	1.489(11)	N(3)–Pd	1.979(12)
Br(1)–Pd–Br(2)	91.87(8)	Br(1)–Pd–N(3)	86.6(3)
N(3)–Pd–N(1)	94.51(46)	N(1)–Pd–Br(2)	87.08(35)
Pd–N(1)–S(1)	132.67(78)	N(1)–S(1)–N(2)	119.79(70)
S(1)–N(2)–S(2)	120.79(78)	N(2)–S(2)–N(3)	122.06(72)
S(2)–N(3)–Pd	129.10(69)		

Table 5 Atomic coordinates for complex **2b**

Atom	x	y	z
Pd	0.471 06(10)	-0.094 02(10)	0.696 08(9)
Br(1)	0.499 1(2)	-0.215 3(2)	0.822 2(2)
Br(2)	0.655 0(1)	-0.061 4(2)	0.713 0(1)
S(1)	0.357 5(4)	0.046 6(4)	0.540 0(3)
S(2)	0.237 4(4)	-0.091 6(4)	0.608 6(3)
P	0.201 5(3)	0.044 5(3)	0.902 8(3)
N(1)	0.450 9(9)	0.007 4(9)	0.603 1(8)
N(2)	0.249(1)	-0.003(1)	0.539 6(9)
N(3)	0.324 0(9)	-0.126 0(9)	0.682 7(9)
C(1)	0.312 2(6)	0.085 3(7)	0.859 1(7)
C(2)	0.303 3(6)	0.168 1(7)	0.803 8(7)
C(3)	0.389 4(8)	0.208 0(6)	0.774 8(6)
C(4)	0.484 5(6)	0.165 2(7)	0.801 0(7)
C(5)	0.493 5(6)	0.082 4(7)	0.856 2(6)
C(6)	0.407 3(8)	0.042 5(6)	0.885 3(6)
C(7)	0.163 0(8)	0.139 4(6)	0.971 5(7)
C(8)	0.064 0(7)	0.175 5(7)	0.951 8(6)
C(9)	0.037 5(6)	0.254 1(7)	1.002 8(7)
C(10)	0.110 0(8)	0.296 7(6)	1.073 4(7)
C(11)	0.209 0(7)	0.260 7(7)	1.093 1(6)
C(12)	0.235 5(6)	0.182 1(7)	1.042 2(7)
C(13)	0.099 8(6)	0.010 5(7)	0.808 2(6)
C(14)	0.086 0(7)	0.051 6(7)	0.715 9(7)
C(15)	0.000 5(8)	0.028 5(7)	0.647 6(5)
C(16)	-0.071 2(6)	-0.035 6(7)	0.671 5(6)
C(17)	-0.057 3(7)	-0.076 8(6)	0.763 8(7)
C(18)	0.028 1(8)	-0.053 7(7)	0.832 2(5)
C(19)	0.230 5(8)	-0.057 2(6)	0.977 8(7)
C(20)	0.204 9(7)	-0.061 1(6)	1.070 9(7)
C(21)	0.217 9(7)	-0.145 0(8)	1.124 2(5)
C(22)	0.256 4(7)	-0.225 1(6)	1.084 4(7)
C(23)	0.282 1(7)	-0.221 2(6)	0.991 3(7)
C(24)	0.269 1(7)	-0.137 3(8)	0.938 0(5)

**Scheme 4** Products of the reaction of complex **2b** with dppe

$[\text{PPh}_4]^+$, the presence of $[\text{Pd}(\text{dppe})(\text{S}_2\text{N}_2)]$, a known complex of $[\text{S}_2\text{N}_2]^{2-}$, together with $[\text{Pd}(\text{dppe})\text{Br}_2]$ (Scheme 4). The reactions also indicate that compound **I** has the potential to react in a similar, but subtly altered, manner to S_4N_4 and suggest that it may well find a variety of synthetic uses. We should, however, add the caveat that it may be that in many reactions it simply mimics S_4N_4 . For example, with the platinum(0) species $[\text{Pt}(\text{PPh}_3)_3]$ the products are $[\{\text{Pt}(\text{S}_2\text{N}_2)(\text{PPh}_3)_2\}_2]$ and $[\text{Pt}(\text{S}_2\text{N}_2)(\text{PPh}_3)_2]$ (Scheme 5), both of which form from S_4N_4 .⁶



Scheme 5 Products of the reaction of compound I with [Pt(PPh₃)₃]

Acknowledgements

We are grateful to Johnson Matthey for loans of precious metals.

References

- 1 T. Chivers and F. Edelmann, *Polyhedron*, 1986, **5**, 1661 and refs. therein.

- 2 P. F. Kelly, A. M. Z. Slawin, D. J. Williams and J. D. Woollins, *Angew. Chem., Int. Ed. Engl.*, 1992, **31**, 616.
- 3 W. Lidy, W. Sundermeyer and W. Verbeek, *Z. Anorg. Allg. Chem.*, 1974, **406**, 228.
- 4 C. P. Warrens and J. D. Woollins, *Inorg. Synth.*, 1989, **25**, 43.
- 5 H. W. Roesky, M. N. S. Rao, T. Nakajima and W. S. Sheldrick, *Chem. Ber.*, 1979, **112**, 3531; T. Chivers, R. T. Oakley, O. J. Scherer and G. Wolmershauser, *Inorg. Chem.*, 1981, **20**, 914; L. Zborilova and P. Gebauer, *Z. Chem.*, 1979, **19**, 32.
- 6 R. Jones, P. F. Kelly, D. J. Williams and J. D. Woollins, *J. Chem. Soc., Chem. Commun.*, 1985, 1325.
- 7 P. A. Bates, M. B. Hursthouse, P. F. Kelly and J. D. Woollins, *J. Chem. Soc., Dalton Trans.*, 1986, 2367.
- 8 TEXSAN, Crystal Structure Analysis Package, Molecular Structure Corporation, Houston, TX, 1985 and 1992.
- 9 V. C. Ginn, P. F. Kelly, A. M. Z. Slawin, D. J. Williams and J. D. Woollins, *J. Chem. Soc., Dalton Trans.*, 1992, 963.
- 10 See, for example, P. F. Kelly, R. N. Sheppard and J. D. Woollins, *Polyhedron*, 1992, **11**, 2605.

Received 10th July 1995; Paper 5/04478B